Translational Oncology 22 (2022) 101461

Contents lists available at ScienceDirect

Translational Oncology

journal homepage: www.elsevier.com/locate/tranon

Original Research

Osimertinib for lung cancer cells harboring low-frequency *EGFR T790M* mutation

Asim Joshi [a,c,#], Ashwin Butle [a,#], Supriya Hait [a,c], Rohit Mishra [a], Vaishakhi Trivedi [b,c], Rahul Thorat [d], Anuradha Choughule [b,c], Vanita Noronha [b,c], Kumar Prabhash [b,c], Amit Dutt [a,c,*]

[a] *Integrated Cancer Genomics Laboratory, Advanced Centre for Treatment Research Education In Cancer (ACTREC), Tata Memorial Centre, Navi Mumbai, Maharashtra, India 410210*

[b] *Department of Medical Oncology, Tata Memorial Centre, Ernest Borges Marg, Parel, Mumbai, India 400012*

[c] *Homi Bhabha National Institute, Training School Complex, Anushakti Nagar, Mumbai, India 400094*

[d] *Laboratory Animal Facility, Advanced Centre for Treatment Research and Education In Cancer (ACTREC), Tata Memorial Centre, Navi Mumbai, Maharashtra, 410210*

ARTICLE INFO

Keywords:
Erlotinib resistance
Low allele fraction EGFR T790M
Osimertinib
Orthotopic lung cancer mice model
Bioluminescence imaging
Next generation sequencing

ABSTRACT

Osimertinib, a third-generation EGFR tyrosine kinase inhibitor, shows significant benefit among patients with *EGFR T790M* mutation at disease progression. We analyzed the whole exome sequence of 48 samples obtained from 16 lung cancer patients with a longitudinal follow-up: treatment-naïve-baseline primary tumors positive for *EGFR* activating-mutations, paired re-biopsies upon disease progression but negative for *EGFR T790M* mutation based on qPCR, and their matched normal blood samples. Our Next generation sequencing (NGS) analysis identified an additional set of 25% re-biopsy samples to harbor *EGFR T790M* mutation occurring at a low-allele frequency of 5% or less, undetectable by conventional qPCR-based assays. Notably, the clinical utility of osimertinib among patients harboring low-allele frequency of *EGFR T790M* in tissue biopsy upon disease progression remains less explored. We established erlotinib-resistant PC-9R cells and twenty single-cell sub-clones from erlotinib-sensitive lung cancer PC-9 cells using *in vitro* drug-escalation protocol. NGS and allele-specific PCR confirmed the low-allele frequency of *EGFR T790M* present at 5% with a 100-fold higher resistance to erlotinib in the PC-9R cells and its sub-clones. Additionally, luciferase tagged PC-9, and PC-9R cells were orthotopically injected through the intercostal muscle into NOD-SCID mice. The orthotopic lung tumors formed were observed by non-invasive bioluminescence imaging. Consistent with *in vitro* data, osimertinib, but not erlotinib, caused tumor regression in mice injected with PC-9R cells, while both osimertinib and erlotinib inhibited tumors in mice injected with PC-9 cells. Taken together, our findings could extend the benefit of osimertinib treatment to patients with low *EGFR T790M* mutation allele frequency on disease progression.

Introduction

Non-small cell lung cancer (NSCLC) is the major cause of cancer-related deaths worldwide [1]. A subset (10% - 35%) of NSCLC patients harbor activating mutations in the epidermal growth factor receptor (*EGFR*) gene [2–5]. The development of EGFR specific small molecule inhibitors, erlotinib and gefitinib, have significantly transformed the standard of care and treatment for these *EGFR*-mutated NSCLC patients. However, in almost all of these patients, the successful application of EGFR tyrosine kinase inhibitors (EGFR-TKIs) is selection and enrichment of cells harboring a single point mutation resulting in a change in amino acid from threonine to methionine at amino acid position 790 in exon 20 of the kinase domain of *EGFR* that contributes to resistance in fifty percent of patients [6, 7]. Osimertinib is a third-generation irreversible EGFR-TKI showing potent activity against both activating and resistant *EGFR* mutations and remains the only approved treatment for NSCLC patients who acquire *EGFR T790M* mutation in response to first-generation EGFR-TKI treatments [8, 9]. Thus, *EGFR T790M* mutation status serves as a predictive marker for osimertinib treatment and routine *EGFR T790M* testing is recommended for

* Corresponding author.
E-mail address: adutt@actrec.gov.in (A. Dutt).
# Equal Contribution

https://doi.org/10.1016/j.tranon.2022.101461
Received 11 February 2022; Received in revised form 17 May 2022; Accepted 18 May 2022

NSCLC patients' progressed on EGFR-TKIs [10] . The ratio of allele fraction of acquired *EGFR T790M* to allele fraction of corresponding *EGFR* activating mutation (L858R or exon 19 deletions), has been associated with poor response to osimertinib [11–15]. However, the clinical utility of osimertinib to low allele fraction of T790M in tissue biopsy remains unexplored. Here, we use a combination of *in vitro* and *in vivo* orthotopic models to present evidence suggesting the potent response of osimertinib treatment on tumor cells harboring low allele frequency *EGFR T790M* mutation.

Materials and methods

Lung cancer cells and EGFR-tyrosine kinase inhibitors

PC-9 and PC-9R cells were cultured aseptically in RPMI-1640 medium (Gibco, Catalog #23400–021) and A549 cells in DMEM medium (Gibco, Catalog #12800–017) and incubated at 37 °C in a 5% CO_2 incubator. The media were supplemented with 10% fetal bovine serum (Catalog 10270–106), 2.5 mg/ml Amphotericin B and 1.5 µl/ml gentamycin (Abbott). The identity of the cells was authenticated using DNA short tandem repeat (STR) profiling kit (Promega, Geneprint 10 system). The cells were routinely tested for mycoplasma and as and when necessary were treated as per the manual of the EZkill mycoplasma elimination kit (HiMedia, Catalog #CK006). EGFR-tyrosine kinase inhibitors erlotinib (Santacruz Biotechnology) and osimertinib (Selleckchem, Catalog #S7297) were used for the experiments. Both PC-9 and PC-9R cells were modified to stably express luciferase by transduction with retroviral construct as described earlier [16]. The EGFR-TKIs were dissolved DMSO for *in vitro* experiments and 10% DMSO in 1X PBS for *in vivo* treatments.

Development of EGFR-TKI resistant cell line model

Erlotinib-resistant PC-9 cells (PC-9R) were established from parental erlotinib-sensitive PC-9 using the *in vitro* drug escalation protocol [17]. Briefly, the PC-9 cells were cultured under increasing concentrations of erlotinib starting from 0.015 µM (IC_{30}) upto 1 µM for a period of about 10–12 months till resistant clones emerged. Once the cells resumed their normal growth at the particular concentration of erlotinib, the concentration was increased in a stepwise manner. PC-9 clones with an ability to survive at 1 µM were considered resistant as described earlier [18]. The identity of the resistant cells PC-9R cells was confirmed by matching the STR profile to parental PC-9 cells and the resistance to erlotinib was confirmed by MTT based cell viability assay.

Generation of single-cell subclones of PC-9R cells

Single-cell subclones of PC-9R were established from the polyclonal PC-9R cells. PC-9R cells were seeded at a density of 0.5 cells/well into 96-well plates. Wells containing only single colonies were marked and allowed to expand. Overall, 20 single-cell subclones of PC-9R were generated and used in further experiments.

Cell viability assay

3×10^3 cells per well were seeded in 96 well plates and incubated overnight. Next day, the inhibitors (erlotinib/osimertinib) were added at various concentrations starting from 0.001 µM till 10 µM through 0.003 µM, 0.01 µM, 0.03 µM, 0.1 µM, 0.3 µM, 1 µM and 3.3 µM. Vehicle-treated cells were used as control. Each concentration of drug was tested in six replicates. 72 h later, the cells were incubated with MTT (HiMedia laboratories, Catalog #TC-191) at concentration of 0.5 mg/ml for three hours. Once the purple precipitate was visible, 100 µl of DMSO was added to all the wells including the controls, and absorbance was measured at 570 nm using a microplate reader. Percentage cell viability at each concentration was calculated against the vehicle-treated cells.

Allele-specific PCR

Allele-specific PCR was performed using quantitative real-time PCR with the following set of primers – wildtype specific forward primer (OAD2434_5′–CACCGTGCAGCTCAGCAC-3′), mutant specific forward primer (OAD2435_5′–CACCGTGCAGCTCAGCAT-3′), and reverse primer (OAD2005_5′- CTTTGCGATCTGCACACAC-3′). Each 6 µl of PCR reaction contained 3 µl SYBR Green master mix, 0.2 µl of forward and reverse primer each, and 10 ng of genomic DNA as a template. PCR reaction was performed at the following conditions: Initial denaturation at 95 °C for 3 min followed by 40 cycles of denaturation (95 °C, 15 s), annealing (60 °C, 15 s), and extension (72 °C, 15 s). 10 ng of genomic DNA was used as a template. Genomic DNA from PC-9, H3255, and A549 cells was used as negative control and H1975 cells were used as a positive control for *EGFR T790M* mutation. The specificity and the sensitivity of both the wild-type specific and mutant specific primers were confirmed by performing real-time PCR using the constructs pBabe-puro-EGFR and pBabe-puro-EGFR T790M at various concentrations including 10 ng, 1 ng, 0.1 ng, 0.01 ng, and 0.001 ng.

Next-generation sequencing for detection of EGFR T790M mutation in cell lines

The raw reads from RNAseq data of PC-9 and PC-9R were mapped to the reference genome (GRCh 38) with two pass modes of STAR aligner (STAR v2.7.6a). These mapped reads were then processed using GATK MarkDuplicates, SplitNCigarReads, and Base Recalibration. These processed reads were then used for variant calling using GATK HaplotypeCaller and Mutect2. The variants called were filtered using SNPiR tool to retain good quality variants [19]. The variants were visualized using an integrative genomics viewer.

Genomic DNA extraction from cell lines and in vivo tissues

Genomic DNA was extracted from cell lines using a QIamp DNA blood mini kit as per the manufacturer's instructions. 0.5×10^6 cells were used for genomic DNA extraction. The flash frozen excised lungs and pleural effusion of mice (stored in RNAlater at −80 °C) was thawed on ice. 150 µl of pleural effusion and 15–20 mg of tumor tissue were used for DNA extraction. Prior to extraction, the lung tissue was chopped and the tissue was homogenized in lysing matrix (MP Biomedicals) with lysis buffer in 1–2 min run of homogenizer (MPBioFastPrep 24). The homogenized tissue was centrifuged at 13,000 rpm for 3 mins and the supernatant was used for DNA extraction. The AllPrep DNA/RNA/miRNA Universal Kit (CatNo. 80,224) was used to elute DNA from the tissue samples while the QIamp DNA blood mini kit was used for pleural effusion. All the procedures were carried out according to the instructions of the respective kits. The concentration and the purity of the DNA were assessed using Nanodrop measurements. The integrity of the genomic DNA was confirmed by running on the gel and by PCR for the *GAPDH* gene.

NOD-SCID mice

The experimental procedures involving animals were reviewed and approved by the Institutional Animal Ethics Committee, ACTREC, Navi-Mumbai, India (Project No. 9/2020). Female NOD-SCID mice (6–8 weeks old) were housed under a specific pathogen-free environment, with a 12-h day-night cycle, in the laboratory animal facility at ACTREC and used for the intercostal implantation of PC-9 and PC-9R cells. The mice were acclimatized to the environmental conditions at least 7 days before use. The animals' health status was monitored throughout the experiments by veterinary health workers in the Animal House Facility of ACTREC. Each mouse was caged for not more than 3 months and the humane endpoint for the experiment was a reduction in the body weight of animals by more than 20%. All the animals were sacrificed with a

lethal dose of CO_2 per the institutional guidelines. At the end of the experiments, the lungs were excised and were fixed with 10% formaldehyde overnight at room temperature, placed in 70% ethanol, and sent for paraffin embedding, sectioning, and hematoxylin and eosin (H&E) staining (Histology Division, ACTREC). Slides were examined histologically to assess the severity of tumor development by a pathologist at ACTREC.

Intercostal implantations into lungs of NOD-SCID mice

Three million cells were resuspended in 70 µl of 1X phosphate-buffered saline with 1.5 mg/ml of matrigel and used for intercostal implantations. The mice were anesthetized in an isofluorane chamber and then positioned in the right lateral decubitus position under a continuous supply of isofluorane through the nasal route. The mice hair was shaved with a hair clipper and the injection site was marked between the fifth and sixth rib bones on the right anterior axillary line. A small incision was made at the marked area and the lower lobe of the left lung was located. Using a 30 G hypodermic needle, the cell suspension was quickly injected at a depth of approximately 5 mm. The incision was closed with a tissue adhesive (3 M Vetbond, 1469SB) and the mice were placed back in the cage and allowed to recover.

Bioluminescence imaging

The formation and progression of tumors were monitored using bioluminescence imaging (Caliper LifeSciences, IVIS Spectrum) at the Molecular Imaging Facility, ACTREC. For bioluminescence imaging (BLI), mice were anesthetized using isofluorane inhalation and injected intraperitoneally with 100 µl of 30 mg/ml of D-luciferin (Carbosynth, L-8220). The luminescence signal was observed using the auto exposure mode in Living Image 4.5 software until the peak was reached. Each mouse was imaged once per week for the duration of the experiment.

Signal intensity was determined by drawing regions of interest (ROIs) around the lung luminescent area of mice. Data were collected in counts (photons/second, p/s) as per manufacturer's instructions, then converted to photons/second/cm^2/steradian (p/s/cm^2/sr) as total photon flux with variable parameters (Exposure time: Auto, F-stop: 1, Binning: medium) used between groups and weeks. Treatment response of EGFR-TKI in orthotopic mouse model was also assessed by $\log_{10}$ fold change, calculated using the $\log_{10}$ of values from the BLI output in response to treatment (p/s/cm^2/sr) or signal at the respective time points of the treatment period subtracted by the $\log_{10}$ of values from BLI signal at the Day 0 value [20].

Determination of EGFR gene alterations by reanalysis of next-generation sequencing data

We reanalyzed an existing next-generation sequencing data of EGFR-TKI sensitive, EGFR-TKI resistant biopsies along with paired blood longitudinally obtained from 16 lung adenocarcinoma patients, whose tumors initially regressed and eventually progressed on EGFR-TKI therapy but remained *EGFR T790M* negative (unpublished data).

Raw Fastq files of each sample were mapped on the human reference genome (GRCh37) and the reads specifically mapping to the exonic region of the *EGFR* gene were extracted and converted to a bam file. The bam file was then used for checking fixmate read information and marking duplicates followed by the base recalibration using GATK v4.1.8. For probing alterations in the *EGFR* gene, variant callers, GATK Haplotype caller, and Mutect2 with interval bed file consisting coordinates of 28 exons of *EGFR* were used (Supplementary table S1). All the variants from GATK HaplotypeCaller were depleted against the paired normal samples. Additionally, only variants from both the callers qualifying the filter of total depth (DP) >= 5 (minimum 5 reads supporting the position) were merged using Bcftools v1.9. These variants were further annotated by Funcotator and subjected to the functional prediction score analysis using 7 different tools by dbNSFP (version 4.0a). All the mutations were further visualized and confirmed using IGV (Integrative Genomics Viewer v2.8.2)

Development of EGFR-TKI resistant orthotopic lung cancer mouse model

The orthotopic lung cancer model was developed by injecting NOD-SCID mice ($n = 3$) with 3×10^6 PC-9-Luciferase tagged cells. Successful injection of cells through the intercostal muscles and the progression of tumors was monitored by bioluminescence imaging (BLI) once per week till the emergence of signs and symptoms of clinical lung cancer. The tumors were excised and histologically confirmed using H&E staining. For therapeutic study, the NOD-SCID mice were randomized into six groups as follows: A) PC-9 luciferase implanted mice treated with vehicle ($n = 3$) B) PC-9R luciferase implanted mice treated with vehicle ($n = 3$) C) PC-9 luciferase implanted mice treated with erlotinib ($n = 3$) D) PC-9 luciferase implanted mice treated with osimertinib ($n = 3$) E) PC-9R luciferase implanted mice treated with erlotinib ($n = 3$) and F) PC-9R luciferase implanted mice treated with osimertinib ($n = 3$). Erlotinib (25 mg/kg) and osimertinib (15 mg/kg) were administered orally daily starting one-week post-injection of cells. Tumors were monitored once per week using BLI and the experiment was continued till the mice in the control groups had to be sacrificed.

Results

Next-generation sequencing data identifies EGFR T790M mutations at low allele frequency in re-biopsies upon disease progression

To assess the prevalence of low-allele *EGFR T790M* mutation in primary tumors, we re-analyzed the next-generation sequencing data of baseline, repeat biopsy, and paired blood samples collected from a total of 16 *EGFR* mutated NSCLC patients whose tumors showed an initial response to first-generation EGFR-TKI treatment followed by progression on the same TKI treatment but remained *EGFR T790M* negative (unpublished data). The NGSCheckMate based analysis revealed 13 of 16 patients as correctly matched sensitive-resistant-blood DNA samples while 2 patients had matched resistant-blood DNA samples [21]. The clinico-pathological details of lung cancer patients analysed in the study has been detailed in Supplementary table S2. Interestingly, the *EGFR*-activating mutations present at baseline, including both L858R and exon 19 deletion were identified in all but one re-biopsy sample following disease progression. Despite a negative result for *EGFR T790M* based on real-time PCR of re-biopsy samples, the NGS data analysis identified the presence of *EGFR T790M* mutations at a low allele frequency (range: 4% - 6%) in an additional 4 of 15 samples (Fig. 1). Owing to the negative *EGFR T790M* outcome-based in real-time PCR, these patients received standard cytotoxic chemotherapy as opposed to osimertinib.

Establishment of PC-9R lung cancer cells resistant to EGFR-TKI erlotinib

To model the development of EGFR-TKI resistance as observed in clinics, we developed erlotinib resistant PC-9R cells from erlotinib sensitive PC-9 cells using an *in vitro* dose escalation protocol. The IC_{50} of erlotinib in PC-9R (2 µM) was 100 folds higher than the IC_{50} of erlotinib in PC-9 (20 nM), thus confirming the acquisition of erlotinib resistance (Fig. 2A). The identical STR profile of PC-9 and PC-9R cells and retention of *EGFR exon 19* deletion in the PC-9R cells confirmed the resistant cells were a derivative of the PC-9 cells. Interestingly, Sanger sequencing of exon 20 regions in PC-9R cells did not show the presence of T790M mutation. However, whole transcriptome analysis of the PC-9R cells identified *EGFR T790M* mutation at a low allele frequency of 5% that was absent in the PC-9 cells (Fig. 2B; Fig. 2C). Furthermore, allele-specific PCR confirmed the presence of *EGFR T790M* mutation in PC-9R cells (Fig. 2C). Next, to test if the mutant allele is encoded by

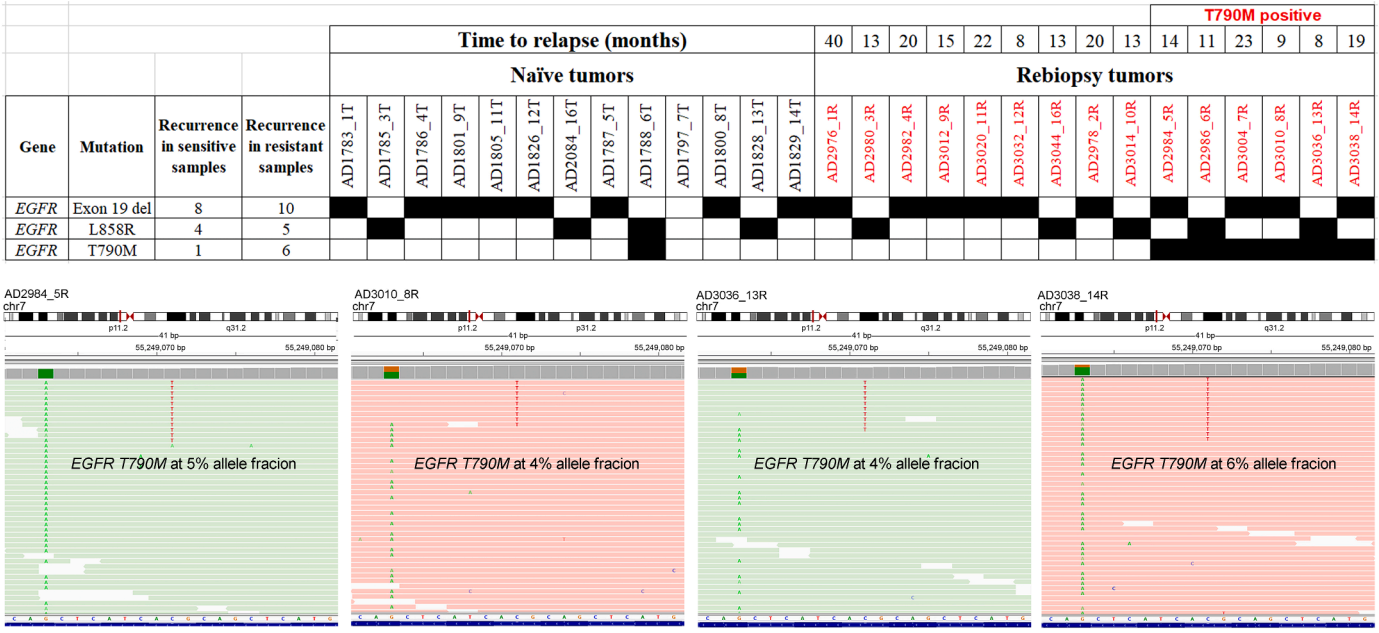

Fig. 1. Analysis of next generation sequencing data of 16 EGFR TKI resistant patients. A) Heatmap showing the *EGFR* activating and resistant mutations in baseline and rebiopsy samples respectively. The black solid boxes indicate the presence of mutation. The time to relapse in months, is mentioned on the top of the heatmap. The IDs mentioned in the black font indicate sensitive patients while those in the red font indicate resistant patients. Integrated genome viewer snapshots of low allele fraction *EGFR T790M* mutations obtained in 4 patients.

extrachromosomal DNA, marked by uneven segregation [22], we performed a serial dilution of the polyclonal PC-9R cells and isolated 20 viable single cell subclones of PC-9R cells. All the single-cell subclones derived from the PC-9R cells maintained *EGFR T790M* at a low allele fraction as validated by allele-specific real-time PCR (Supplementary Figure S1), suggesting the acquired mutant allele was stably encoded by the chromosomal DNA. All the 20 single cell subclones retained resistance to erlotinib (Supplementary Figure S2). The resistance of polyclonal PC-9R cells was retained following its long-term culture (>12 months) in an erlotinib free medium, driven by the secondary chromosomal *EGFR T790M* mutation. We then tested the IC_{50} of polyclonal PC-9R cells to third-generation EGFR-TKI osimertinib, a potent and selective inhibitor of both EGFR-TKI sensitizing mutation and *EGFR T790M* resistance mutations. While PC-9, but not PC-9R cells, were sensitive to erlotinib, both were inhibited by osimertinib with a comparable IC_{50} of 18 nM (Fig. 2A).

Erlotinib resistant tumors harboring EGFR T790M at low allele frequency retain sensitivity to osimertinib, in vivo

Next, to test the relevance of *EGFR T790M* at low allele frequency in resistance and to establish sensitivity to osimeritinb, we established orthotopic lung cancer mouse model. Polyclonal population of PC-9R cells was used for *in vivo* studies. Three million PC-9 and PC-9R cells were used for intercostal implantations in 18 NOD-SCID mice randomized into six groups of three mice, each. None of the mice across all the groups died during the surgical procedure of intercostal implantation. The successful implantation of the cells was confirmed with BLI after 2 h of intercostal implantation and all the mice in the respective groups showed luminescence signal. Thirty days after implantation, mice showed remarkably decreased activities, shortness of breath, and poor response to external stimuli. Further, to assess the severity of the disease, a pulmonary assessment of advanced metastasis (PAAM) test, was performed by restraining the individual mouse and gently applying pressure under the xiphoid process to reduce the diaphragmatic component to respiration [23]. The mice showed transient signs of respiratory distress by opening their mouth and pursed lips within 3 s of the application of this pressure with a finger. Additionally, mice showed an increase in luminescence (photons/second) starting from day 10 (Fig. 3A). The tumor-bearing mice showed clinical symptoms of the disease after day 30 and were euthanized with a lethal dose of CO_2. The mice were dissected and the pleural cavities were exposed through longitudinal chest incisions at the mid-clavicular lines. Lungs were excised and gross observation showed that the whole thorax of all mice was entirely occupied with free-floating bilateral malignant pleural effusion and massive tumor growth in the left lungs was clearly visible. The metastatic foci were also observed in the mediastinal, contralateral, and pleural regions (Fig. 3B). The luminescence signal from excised lungs and the pleural effusion collected from the pleural cavity of mice confirmed the presence of malignant cells and tumor colonies respectively. Additionally, minute metastatic lung colonies were also observed in the other lobes of the lung (Fig. 3C) . The orthotopic tumors were confirmed by H&E staining which showed tumor cell nodules with distinct edges in the lobes of the lung as shown in Fig. 3D . Moreover, lung parenchymal inflammation and inflammatory cell influx were remarkable in all three PC-9 luciferase cell implanted mice.

In the vehicle control group, both the PC-9 and PC-9R implanted mice were orally administered with 10% DMSO in 1X PBS. All the three mice in the control PC-9 and PC-9R groups showed a comparable increase in $\log_{10}$ fold change of the bioluminescence intensity [20] over a period of time and were sacrificed at day 56 and day 63 respectively after humane endpoints were reached (Fig. 4). The erlotinib and osimertinib treatments were given daily through the oral administration route at the doses of 25 mg/kg and 15 mg/kg respectively, as described earlier [16]. In the erlotinib receiving PC-9 implanted mice, two of the three mice showed a significant decrease in the luminescence signal continuously after initiation of the treatment observed in signals relative to the basal level (signal intensity at Day 0) in two of PC-9-luciferase cell implanted mice (−2.84 & −0.13) while in other mice it was very little increase as 0.68 but observed decrease in bioluminescence signal from the peak of day 35 as −0.69. Interestingly, fold changes in bioluminescence signals increased even in presence of erlotinib treatment in all three PC-9R-luciferase cell implanted mice 1.38, 2.91, and 0.58 respectively (Fig. 4), thus indicating the progression of tumors on

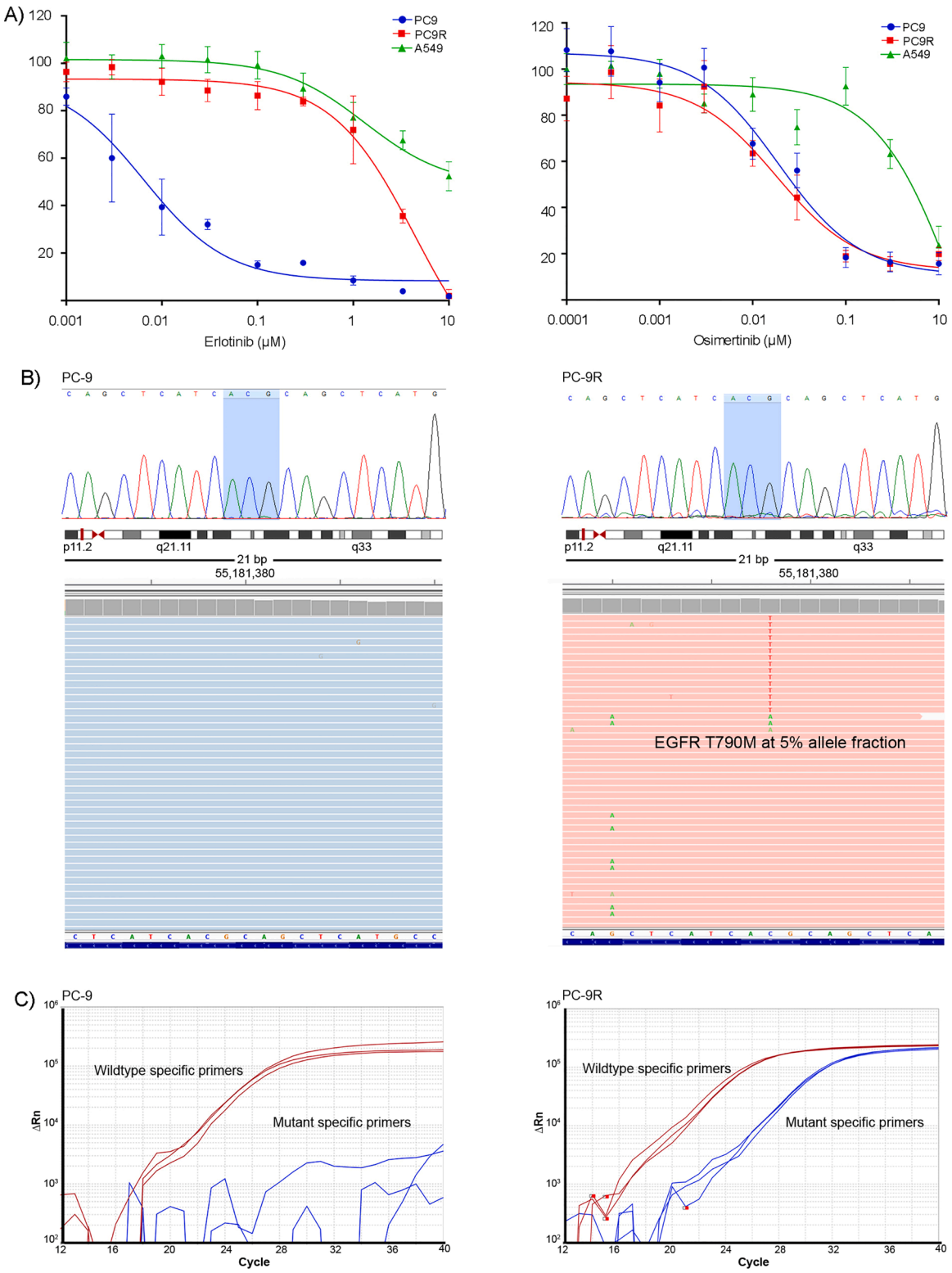

Fig. 2. Establishment and characterization of erlotinib-resistant PC-9R cells. A) MTT assay for assessing the response of PC-9R cells (red) to EGFR-TKIs. PC-9 (blue) was used as sensitive control for EGFR-TKIs and A549 cells (green) were the resistant control. The percentage of cells surviving the treatment is plotted on the y-axis and the drug concentration on the x-axis. B) Sanger sequencing traces for *EGFR T790M* in PC-9 (left) and PC-9R cells (right). In both PC-9 and PC-9R cells, *EGFR T790M* mutation could not be detected by Sanger sequencing (top panel). The bottom panel shows detection of low-frequency *EGFR T790M* mutation using variant calls from the transcriptome sequencing data. An integrated genome viewer was used to visualize the mutation. Low allele frequency *EGFR T790M* mutation was observed in PC-9R cells. C) Validation of EGFR T790M mutation by allele specific PCR in PC-9 (left) and PC-9R cells (right). The amplification plots for allele specific real time PCR performed using primers specifically amplifying the wild type allele (red) and mutant allele (blue) are shown. The red curves indicate the presence of threonine (T) at amino acid 790 and blue curves indicate the presence of amino acid methionine (M) at position 790.

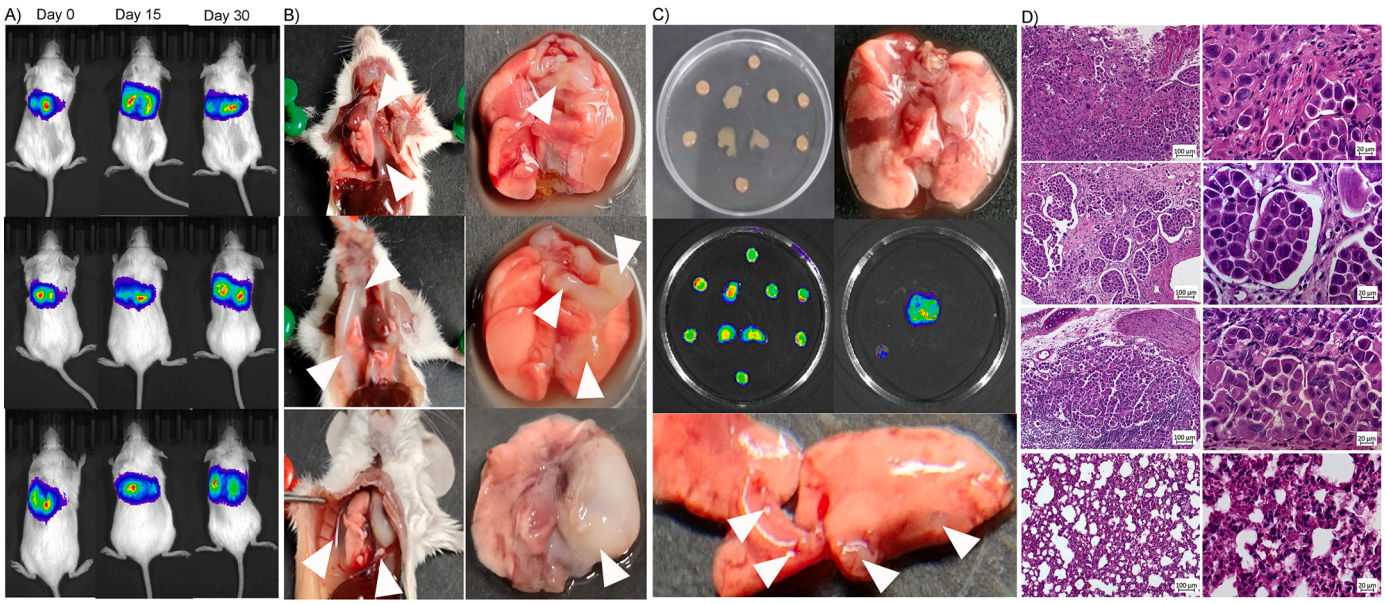

Fig. 3. Orthotopic mouse model system established using PC-9 luciferase cells simulates the clinical condition of lung cancer. A) 3×10^6 PC-9 luciferase cells were injected into the lower lobe of left lung of NOD-SCID mice ($n = 3$) through intercostal implantation. Bioluminescence imaging was used to monitor the tumor growth of each mice. Representative images (in rows) for three mice are shown at day 0, day 15 and day 30. B) The terminal dissection of the three mice showed presence of extensive pleural effusion (white arrowheads). The adjoining images (right panel) depict the massive tumor growth in the lungs excised from these mice (white arrowheads). C) Representative images showing the collected pleural effusion and excised lungs in petri dish (top row). The corresponding bioluminescence images for the pleural effusion and excised lungs are shown (middle row) confirms the presence of malignant cells and tumors from PC-9 luciferase cells. The bottom row shows the magnified image of mouse's right lung lobes. The metastatic colonies observed in these lobes are indicated by white arrowheads. D) H&E staining was performed to confirm the presence of tumors in the lungs of three mice. The 100X and 400X microscopic images of the tumors from each of the three mice are shown adjacent to each other (upper three rows). The bottom row shows the H&E image of lung excised from healthy mice.

erlotinib. One mice in the PC-9R group died because of severe disease symptoms on day 42 post-implantation of cells while still on erlotinib. In accordance with the *in vitro* data and literature supporting the higher efficacy of osimertinib, both the PC-9 and PC-9R mice showed remarkable responses to daily osimertinib treatment. In mice treated with osimertinib, $\log_{10}$ BLI fold change decreased from the basal level in both PC-9 and PC-9R luciferase implanted mice by order of −4.75, −2.42 and −1.38, while, −1.85, −1.77, and −0.93 respectively. Post completion of the duration of *in vivo* treatments, the mice were sacrificed and lung tumors and/or pleural effusion were collected for genomic DNA extraction from the mice in the PC-9 and PC-9R control group and erlotinib treated PC-9R group. Allele-specific PCR performed on genomic DNA confirmed the presence of *EGFR T790M* mutation in the PC-9R group.

Discussion

EGFR mutated lung cancer patients with an initial clinical response to first generation EGFR-TKIs treatment (such as gefitinib and erlotinib), eventually develop resistance to EGFR-TKIs. Multiple mechanisms of acquired resistance have been described such as the secondary mutations in EGFR including *EGFR T790M*, reactivation of the EGFR pathway due to mutations in downstream molecules like RAS or RAF, bypass pathway activation including *MET* amplification, *ERBB2* amplification, *IGF1R* amplification, *PTEN* loss and activation of AXL kinase among few others and the phenotypic switching including small cell transformation and epithelial to mesenchymal transition [24]. The prevalence of the *EGFR T790M* among NSCLC patients ranges from one-half to three-fourths of re-biopsy samples following disease progression, with a varying allele frequency depending on the sensitivity of the assay [25,26]. Recent studies indicate relative allele fraction (RAF) of T790M, the ratio of T790M to *EGFR*-sensitizing mutation allele frequency, in plasma represent a prognostic stratification with low T790M RAF (<20%) as a contraindication for osimertinib treatment [11–15]. However, the clinical utility of osimertinib to low allele fraction of T790M in tissue biopsy remains unexplored.

To model the typical clinical scenario of *EGFR* mutated lung cancer patients treated with erlotinib, *in vitro*, we treated the PC-9 cells harboring *EGFR exon 19* deletion with erlotinib until erlotinib resistant PC-9R cells were derived. The low frequency of *EGFR T790M* mutation in the PC-9R cells was validated by NGS and allele-specific real-time PCR. Interestingly, the PC-9R cells harbored *EGFR T790M* mutation at an allele fraction of 5% and a relative allele frequency (ratio of T790M allele frequency to E746_A750 allele frequency) of 10% but showed sensitivity to osimertinib comparable to PC-9 with an IC50 value of 18 nM. We additionally isolated 20 single cell subclones of PC-9R cells, all of which retained the *EGFR T790M* at a low allele fraction suggesting chromosomal mutation in the PC-9R cells. To assess the response of erlotinib and osimertinib on PC-9 and PC-9R *in vivo*, we tagged both PC-9 and PC-9R cells with luciferase to allow BLI monitoring of these cells when injected in mice following their intercostal implantation into the lobe of the left lung of NOD-SCID mice. The orthotopic mouse model closely followed the clinical progression of lung cancer as observed in patients as evident by the clinical signs and symptoms as confirmed by PAAM test [23], development of distinct tumor nodules along the edges of the lung, and observation of extensive malignant pleural effusion in the mice not subjected to any treatment. Next, we orally administered erlotinib and osimertinib to mice bearing tumors and tracked the response of tumors using BLI. Indeed, mice in the PC-9-luciferase group showed reduction following treatment with both erlotinib and osimertinib while tumors in the PC-9R-luciferase group responded only to osimertinib. Allele-specific PCR on tumors obtained from PC-9R injected control and erlotinib treatment group revealed the presence of low-frequency *EGFR T790M* mutation thus suggesting no clonal selection of *EGFR T790M* clones in the lung of mice.

Most importantly, our mutation analysis of EGFR TKI resistant re-biopsy patient samples identified the acquisition of low allele *EGFR T790M* mutations in 4 of 15 samples that were missed by real-time PCR.

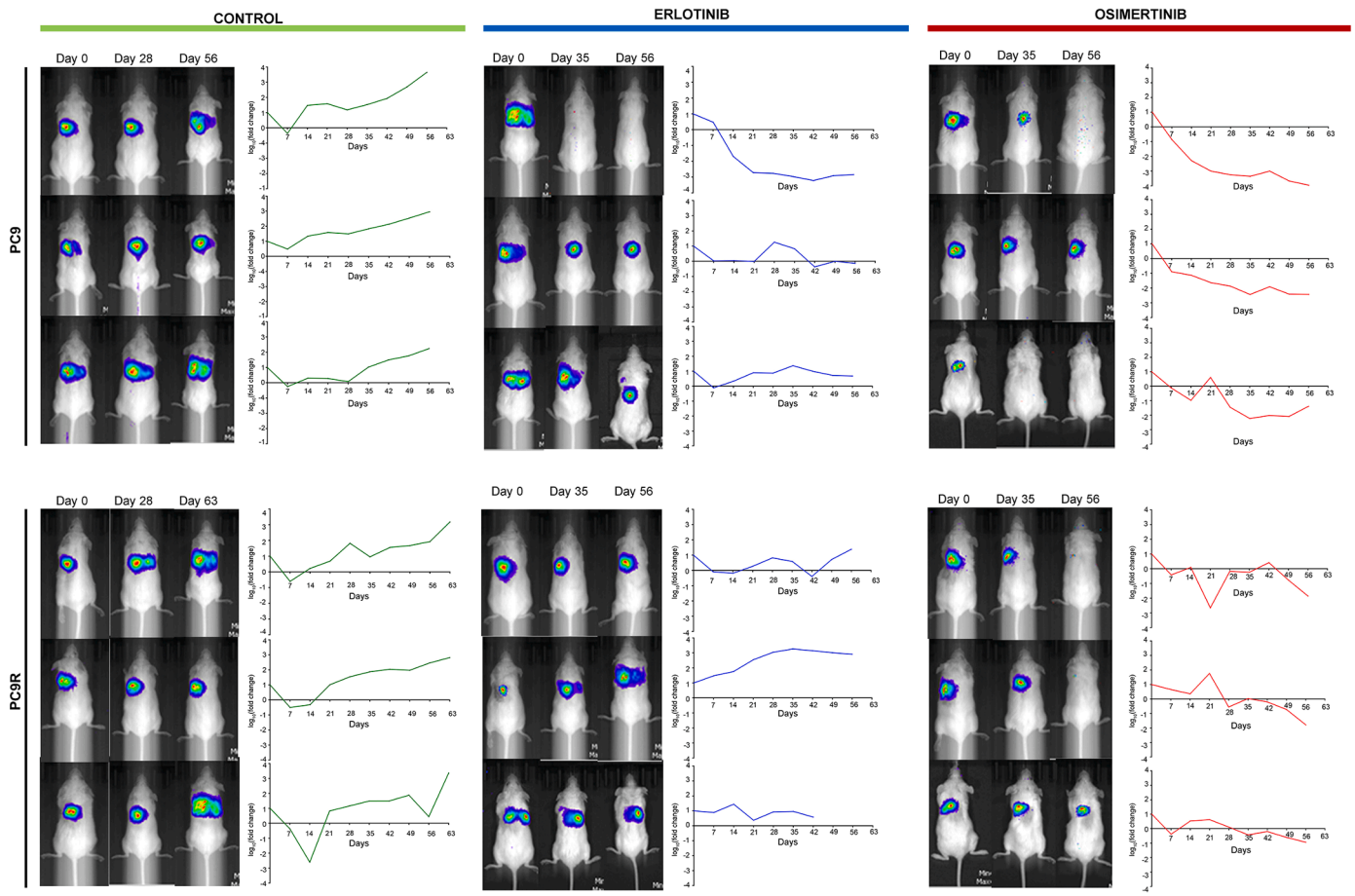

Fig. 4. Recapitulation of in *vitro* EGFR-TKI response in orthotopic lung cancer mouse model. 3×10^6 PC-9 ($n = 9$) and PC-9-R ($n = 9$) cells were subjected to intercostal implantation in NOD-SCID mice and grouped for the daily treatment as control, erlotinib, and osimertinib ($n = 3$ each group). The adjacent graph shows the bioluminescence of each mouse taken at an interval of 7 days. In the control group (left panel) of PC-9 and PC-9R implanted mice, all mice show a continuous increase in lung bioluminescence till days 56 and 63 respectively. In the erlotinib treated group (middle panel), PC-9 cells implanted mice showed steady ($n = 2$) or reduction ($n = 1$) in lung bioluminescence while the PC-9R implanted mice group showed an increase in bioluminescence. In the osimertinib treated group (right panel), both PC-9 and PC-9-R implanted mice show a reduction in lung bioluminescence except single mice implanted with PC-9 cells show increased bioluminescence at day 63.

Thus, real-time PCR performed on FFPE samples under clinical settings could result in false-negative identification of *EGFR T790M* mutations occurring at low allele frequency. Similar results were obtained by Masago et al. wherein *EGFR T790M* mutations, with allele fraction in the range of 4.8% – 7.3% failed to be detected in 3 of 15 patients by conventional methodology but were detected by next-generation sequencing [27]. In another study by Lee *et al.* 2 of 12 *EGFR T790M* positive patients acquired the mutation with an allele frequency of 5% - 7% [28]. Notably, 2 of 9 patients harboring *EGFR T790M* mutation at an allele fraction of 2.2% and 4.6% showed a progression-free survival of 20 and 13 months respectively with Osimertinib [29], consistent with our *in vitro* and *in vivo* results of osimertinib response on low allele frequency *EGFR T790M* mutations. Similarly, studies with real-life data, including the FLAURA trial, indicate the benefit of osimertinib to about 25–31% among patients with relapse harboring *EGFR T790M* mutation compared to those who receive osimertinib as the first subsequent therapy due to rapid disease progression [6, 7, 30]. Nonetheless, this may be an underestimation due to the occurrence of *EGFR T790M* at low allele frequency as a false negative, with additional patients who could benefit from the treatment with osimertinib.

In summary, our findings suggest that the frequency of *EGFR T790M* mutation among patients following disease progression on TKI is likely higher than previously reported, with the inclusion of mutations occurring at allele frequency. Additionally, we show an extended benefit of osimertinib treatment to these patients with low *EGFR T790M* mutation allele frequency, following relapse.

Funding

This work was supported by an extramural grant from SERB-DST (EMR/2016/007218) to A.D. The funders had no role in study design, data analysis, decision to publish and preparation of the manuscript.

Ethics approval

All the experimental procedures performed in this study followed ethical guidelines for animal studies and were reviewed and approved by the Institutional Animal Ethical Committee of ACTREC (Proposal No. 9/2020)

Data availability statement

The raw next generation sequencing data for all the samples is available on ArrayExpress under the accession number E-MTAB-11404.

CRediT authorship contribution statement

Asim Joshi: Conceptualization, Investigation, Formal analysis,

Writing – original draft. **Ashwin Butle:** Conceptualization, Investigation, Formal analysis, Writing – original draft. **Supriya Hait:** Investigation, Formal analysis. **Rohit Mishra:** Investigation, Formal analysis. **Vaishakhi Trivedi:** Investigation. **Rahul Thorat:** Formal analysis. **Anuradha Choughule:** Formal analysis. **Vanita Noronha:** Formal analysis. **Kumar Prabhash:** Formal analysis. **Amit Dutt:** Conceptualization, Investigation, Formal analysis, Resources, Writing – original draft, Project administration, Funding acquisition.

Declaration of interests

The authors declare that they have no known competing financial interests or personal relationships that could have appeared to influence the work reported in this paper.

Acknowledgements

All the members of Dutt Laboratory for critically reviewing the manuscript. Molecular Imaging Facility, ACTREC for helping with the bioluminescence imaging of the mice. A.J and S.H are supported by senior research fellowship from ACTREC. A.B is supported by post-doctoral fellowship from ACTREC.

Supplementary materials

Supplementary material associated with this article can be found, in the online version, at doi:10.1016/j.tranon.2022.101461.

References

[1] H. Sung, J. Ferlay, R.L. Siegel, M. Laversanne, I. Soerjomataram, A. Jemal, et al., Global Cancer Statistics 2020: GLOBOCAN Estimates of Incidence and Mortality Worldwide for 36 Cancers in 185 Countries, CA Cancer J. Clin. 71 (3) (2021) 209–249.

[2] Cancer Genome Atlas Research N. Comprehensive molecular profiling of lung adenocarcinoma, Nature 511 (7511) (2014) 543–550.

[3] W. Pao, J Chmielecki, Rational, biologically based treatment of EGFR-mutant non-small-cell lung cancer, Nat. Rev. Cancer 10 (11) (2010) 760–774.

[4] A. Chougule, K. Prabhash, V. Noronha, A. Joshi, A. Thavamani, P. Chandrani, et al., Frequency of EGFR mutations in 907 lung adenocarcioma patients of Indian ethnicity, PLoS One 8 (10) (2013) e76164.

[5] P. Chandrani, K. Prabhash, R. Prasad, V. Sethunath, M. Ranjan, P. Iyer, et al., Drug-sensitive FGFR3 mutations in lung adenocarcinoma, Ann. Oncol. 28 (3) (2017) 597–603.

[6] J. Chmielecki, J. Foo, G.R. Oxnard, K. Hutchinson, K. Ohashi, R. Somwar, et al., Optimization of Dosing for EGFR-Mutant Non–Small Cell Lung Cancer with Evolutionary Cancer Modeling, Sci. Transl. Med. 3 (90) (2011) 90ra59.

[7] V. Noronha, A. Choughule, V. Patil, A. Joshi, R. Kumar, D. Susan Joy Philip, et al., Epidermal growth factor receptor exon 20 mutation in lung cancer: types, incidence, clinical features and impact on treatment, Onco Targets Ther 10 (2017) 2903–2908.

[8] J.C. Soria, Y. Ohe, J. Vansteenkiste, T. Reungwetwattana, B. Chewaskulyong, K. H. Lee, et al., Osimertinib in Untreated EGFR-Mutated Advanced Non-Small-Cell Lung Cancer, N. Engl. J. Med. 378 (2) (2018) 113–125.

[9] V.A. Papadimitrakopoulou, T.S. Mok, J.Y. Han, M.J. Ahn, A. Delmonte, S. S. Ramalingam, et al., Osimertinib *versus* platinum-pemetrexed for patients with EGFR T790M advanced NSCLC and progression on a prior EGFR-tyrosine kinase inhibitor: AURA3 overall survival analysis, Ann. Oncol. 31 (11) (2020) 1536–1544.

[10] P.A. Jänne, J.C.-.H. Yang, D-W Kim, D. Planchard, Y. Ohe, S.S. Ramalingam, et al., AZD9291 in EGFR Inhibitor–Resistant Non–Small-Cell Lung Cancer, N. Engl. J. Med. 372 (18) (2015) 1689–1699.

[11] T. Vaclova, U. Grazini, L. Ward, D. O'Neill, A. Markovets, X. Huang, et al., Clinical impact of subclonal EGFR T790M mutations in advanced-stage EGFR-mutant non-small-cell lung cancers, Nat. Commun. 12 (1) (2021) 1780.

[12] G.R. Oxnard, K.S. Thress, R.S. Alden, R. Lawrance, C.P. Paweletz, M. Cantarini, et al., Association Between Plasma Genotyping and Outcomes of Treatment With Osimertinib (AZD9291) in Advanced Non–Small-Cell Lung Cancer, J. Clin. Oncol. 34 (28) (2016) 3375–3382.

[13] A. Buder, M.J. Hochmair, M. Filipits, The Allele Frequency of EGFR Mutations Predicts Survival in Advanced EGFR T790M-Positive Non-small Cell Lung Cancer Patients Treated with Osimertinib, Target Oncol 16 (1) (2020) 77–84.

[14] R. Ariyasu, S. Nishikawa, K. Uchibori, T. Oh-hara, T. Yoshizawa, Y. Dotsu, et al., High ratio of T790M to EGFR activating mutations correlate with the osimertinib response in non-small-cell lung cancer, Lung Cancer 117 (2018) 1–6.

[15] Y. Wang, Y. He, P. Tian, W. Wang, K. Wang, S. Chuai, et al., Low T790M relative allele frequency indicates concurrent resistance mechanisms and poor responsiveness to osimertinib, Transl. Lung Cancer Res. 9 (5) (2020) 1952–1962.

[16] A. Butle, A. Joshi, V. Noronha, K. Prabhash, A. Dutt, Weekly osimertinib dosing prevents EGFR mutant tumor cells destined to home mouse lungs, Transl. Oncol. 14 (8) (2021), 101111.

[17] J.A. Engelman, K. Zejnullahu, T. Mitsudomi, Y. Song, C. Hyland, J.O. Park, et al., MET amplification leads to gefitinib resistance in lung cancer by activating ERBB3 signaling, Science 316 (5827) (2007) 1039–1043.

[18] J.A. Engelman, T. Mukohara, K. Zejnullahu, E. Lifshits, A.M. Borras, C.M. Gale, et al., Allelic dilution obscures detection of a biologically significant resistance mutation in EGFR-amplified lung cancer, J. Clin. Invest. 116 (10) (2006) 2695–2706.

[19] R. Piskol, G. Ramaswami, B. Li Jin, Reliable Identification of Genomic Variants from RNA-Seq Data, Am. J. Human Genetics 93 (4) (2013) 641–651.

[20] L. Jones, J. Richmond, K. Evans, H. Carol, D. Jing, R.T. Kurmasheva, et al., Bioluminescence Imaging Enhances Analysis of Drug Responses in a Patient-Derived Xenograft Model of Pediatric ALL, Clin. Cancer Res. 23 (14) (2017) 3744–3755.

[21] S. Lee, S. Lee, S. Ouellette, W.-.Y. Park, E.A. Lee, P.J. Park, NGSCheckMate: software for validating sample identity in next-generation sequencing studies within and across data types, Nucleic. Acids. Res. 45 (11) (2017) e103-e.

[22] X. Gu, J. Yu, P. Chai, S. Ge, X. Fan, Novel insights into extrachromosomal DNA: redefining the onco-drivers of tumor progression, J. Exp. Clin. Cancer Res. 39 (1) (2020) 215.

[23] A. Mendoza, R. Gharpure, J. Dennis, J.D. Webster, J. Smedley, C. Khanna, A novel noninvasive method for evaluating experimental lung metastasis in mice, J. Am. Assoc. Lab. Anim. Sci. 52 (5) (2013) 584–589.

[24] D. Westover, J. Zugazagoitia, B.C. Cho, C.M. Lovly, Paz-Ares L. Mechanisms of acquired resistance to first- and second-generation EGFR tyrosine kinase inhibitors, Ann. Oncol. 29 (2018) i10. -i9.

[25] T.K. Sundaresan, L.V. Sequist, J.V. Heymach, G.J. Riely, P.A. Jänne, W.H. Koch, et al., Detection of T790M, the Acquired Resistance EGFR Mutation, by Tumor Biopsy *versus* Noninvasive Blood-Based Analyses, Clin. Cancer Res. 22 (5) (2016) 1103–1110.

[26] Y. Li, F. Zhang, P. Yuan, L. Guo, Y. Jianming, J. He, High MAF of EGFR mutations and high ratio of T790M sensitizing mutations in ctDNA predict better third-generation TKI outcomes, Thorac Cancer 11 (6) (2020) 1503–1511.

[27] K. Masago, S. Fujita, M. Muraki, A. Hata, C. Okuda, K. Otsuka, et al., Next-generation sequencing of tyrosine kinase inhibitor-resistant non-small-cell lung cancers in patients harboring epidermal growth factor-activating mutations, BMC Cancer 15 (1) (2015) 908.

[28] C-k Lee, S. Kim, J.S. Lee, J.E. Lee, S-m Kim, I.S. Yang, et al., Next-generation sequencing reveals novel resistance mechanisms and molecular heterogeneity in EGFR-mutant non-small cell lung cancer with acquired resistance to EGFR-TKIs, Lung Cancer 113 (2017) 106–114.

[29] K. Nie, H. Jiang, C. Zhang, C. Geng, X. Xu, L. Zhang, et al., Mutational Profiling of Non-Small-Cell Lung Cancer Resistant to Osimertinib Using Next-Generation Sequencing in Chinese Patients, Biomed. Res. Int. 2018 (2018) 1–6.

[30] S.S. Ramalingam, J. Vansteenkiste, D. Planchard, B.C. Cho, J.E. Gray, Y. Ohe, et al., Overall Survival with Osimertinib in Untreated, EGFR-Mutated Advanced NSCLC, N. Engl. J. Med. 382 (1) (2020) 41–50.